



OPEN A dynamic framework of brain functional patterns shaped by spontaneous thoughts beyond the default mode network

Sandrine Cremona✉, Achille Gillig, Emmanuel Mellet & Marc Joliot

Cognitive functions emerge from the dynamic interplay of distributed, large-scale brain networks. Functional connectivity (FC) reflects stable brain organization and general cognitive abilities, while also capturing individual variations in transient cognitive states. Analyzing data from 1,717 participants, we show that rich and diverse spontaneous thought profiles align with distinct patterns of functional network integration. Evocative profiles were linked to the integration of self-awareness, executive, and visual networks; vigilant profile to salience and sensorimotor networks integration; and fluctuating profile to executive networks integration. Conversely, visual and verbal-predominant profiles were associated with the segregation of visual and language networks, respectively. Covering the full spectrum of observed spontaneous thought profiles, these findings reconceptualize the resting-state as a dynamic, distributed pattern of FC, varying across individuals and defined by the intricate balance of functional network integration and segregation, rather than a simple 'default mode network.'

Modern human neuroscience demonstrates that cognitive and behavioral functions emerge from the dynamic interactions of distributed and interconnected brain networks^{1,2}. Functional connectivity (FC), defined as the spontaneous coactivity of distinct brain regions, is typically studied using resting-state functional magnetic resonance imaging (rfMRI), which measures spontaneous BOLD fluctuations in the absence of external task demands³. A seminal shift occurred in the early 2000s with the discovery of the default mode network (DMN), a set of brain regions more active at rest than during task execution, and strongly involved in self-referential, introspective, and memory-related processes^{4,5}. Since then, research has consistently revealed stable and replicable patterns of intrinsic brain organization, collectively referred to as resting-state networks, which closely resemble the brain's task-evoked architecture^{6–8}. These networks are now considered a core scaffold supporting human cognition⁹, capable of predicting individual differences in task performance^{10,11} and evoked brain activity¹².

Resting-state networks show remarkable anatomical consistency, with large-scale parcellations identifying up to 98 distinct networks^{13–16}. However, efforts to standardize these^{17–22} have led to the convergence around a more tractable set of core functional networks (typically 5–8 systems)^{13,16,21,23,24}. These include the DMN, associated with self-reference, memory, and social cognition²⁵; several executive control networks^{26,27} such as the salience network (SN), involved in filtering salient stimuli and integrating sensory, emotional, and cognitive information²⁸; the frontoparietal network (FPN), supporting flexible cognitive control^{29,30}; the dorsal attention network (DAN), specialized in visuospatial attention^{31,32}; and the cingulo-opercular network (CON), implicated in decision-making and conflict monitoring³³. Additional domain-specific systems include the language network (LAN)^{34–36}, the somatomotor network (SMN), supporting sensory-motor and auditory functions, and the visual network (VN), involved in visual processing²¹.

Importantly, beyond reflecting stable neurocognitive traits, resting-state FC also tracks dynamic fluctuations³⁷ in arousal³⁸, autonomic regulation³⁹, and spontaneous mentation⁴⁰. Whole-brain FC patterns can discriminate between distinct mental contents (including autobiographical thought, inner speech, or music imagery^{41,42}) and relate to fluctuations in self-reported experience^{43–45}. This dynamism has prompted a shift from viewing rest as a monolithic state to a more nuanced perspective, in which resting cognition is understood as emerging from the continuous reconfiguration of network coupling. More specifically, it reflects a balance between functional *segregation*, i.e., strong interaction within networks and minimal interaction across them, and functional *integration*, characterized by increased interaction and information exchange between distinct networks⁴⁶.

Univ. Bordeaux, CNRS, CEA, IMN, UMR 5293, 146 rue Léo Saignat, 33000 Bordeaux, France. ✉email: sandrine.cremona@u-bordeaux.fr

Recent work has identified distinct recurring patterns of spontaneous thought at rest measured in large samples through self-report and clustering analyses^{43,47,48}. These resting-state thought profiles (RSTPs) reflect variations in richness, modality, and focus of internal experience. Yet, most studies exploring the neural basis of spontaneous thought at rest have relied on small samples ($N < 300$), and provided only partial insight into how distinct spontaneous thought profiles relate to functional integration and segregation dynamics^{40,43,44,48–50}. To address these limitations, we investigated FC in a large sample of 1,717 participants in relation to spontaneous thought across six previously defined RSTPs⁴⁷: two *Evocative* profiles (*Preoccupied* and *Reverie*), one *Fluctuating*, one *Vigilant*, and two modality-*predominant* profiles (*Visual* and *Verbal*), spanning the full diversity of mental resting-state experience. We hypothesized that sparser thought profiles would be associated with greater network functional segregation, while richer, more complex profiles would involve enhanced network functional integration.

FC changes were interpreted in the specific context of rest. Within-network desynchronization (i.e., decreased FC) was taken as a marker of functional segregation, reflecting more differentiated processing within a given network. Conversely, between-network desynchronization was interpreted as a marker of functional integration, reflecting the flexible coordination and interplay between distinct networks. While increased FC is typically associated with greater functional engagement in studies using delayed cognitive assessments⁵¹, we argue that, during rest, decreased FC may instead reflect the active recruitment of specific networks involved in spontaneous cognitive processes. This interpretation aligns with empirical findings demonstrating that brain regions exhibiting strong task-evoked activity tend to display low intrinsic connectivity at rest, suggesting a functional dissociation between activation and connectivity^{52,53}. Moreover, task-based dynamic FC studies indicate that decreases in FC can reflect context-specific reorganization or the selective engagement of neural populations, rather than simple network disengagement⁵⁴. Specifically, such decreases may support functional specialization⁵⁵ or facilitate selective information routing during cognition⁵⁶. Finally, theoretical models describing resting-state FC as a dynamic system of transient coupling and decoupling, rather than a static scaffold, further support the notion that desynchronization can accompany active cognitive processing^{57–59}.

Our analysis proceeded in two main steps. First, we identified and characterized seven core functional networks using the GINNA atlas, a cognitively annotated functional atlas that enables the identification of functional networks with known psychological correlates¹⁸. Second, we assessed both within- and between-network FC differences across the six RSTPs. These profiles were previously derived using a multidimensional clustering strategy applied to subjective reports of thought content at rest⁴⁷. FC was computed using Fisher's *r*-to-*z* transformed correlation coefficients across all pairwise regions. We analyzed the effects of RSTPs on FC using two mixed-effects models (one for within-network, one for between-network FC), including participant as a random effect.

This approach allowed us to estimate how frequently each core network was implicated in significant FC differences for each RSTP, and which specific connectivity edges defined shared vs. profile-specific patterns of functional integration and segregation. These analyses revealed consistent FC patterns for each spontaneous thought profile, highlighting how network-level reorganization underlies the diversity of spontaneous mental experience at rest.

Results

Core functional brain networks identified from GINNA analysis

To define the brain's core functional networks, we relied on the 32 resting-state cortical networks from the Groupe d'Imagerie Neurofonctionnelle Network Atlas (GINNA)¹⁸. Through hierarchical clustering, we identified seven core functional networks. A key strength of the GINNA atlas lies in its rigorous and cognitively specific annotation of each network, derived through meta-analytic decoding using Neurosynth⁶⁰. This methodology enabled a valid and precise functional labeling of the core networks, firmly anchored in established task-evoked cognitive domains. Crucially, thanks to this pre-existing annotation, the cognitively informed classification of core networks could be established prior to examining their association with spontaneous thought profiles at rest, thereby providing a robust and interpretable framework. The anatomical layout of these networks is depicted in 3D in Fig. 1 and described in detail in the **Methods** section.

Synchronizations and desynchronizations of core functional networks linked to spontaneous thought profiles

In a previous study, we identified and characterized six distinct resting-state thought profiles (RSTPs) using the ReSQ 2.0 self-report questionnaire, a method allowing the estimation of spontaneous thoughts emerging during rfMRI acquisition⁴⁷. In the present study, we used mixed linear regression models to examine variability in between-network and within-network FC across brain core functional networks related to spontaneous thoughts. Fisher's *r*-to-*z* transformed correlation values were computed for 21 between-network edges and for within-network FC, serving as outcome variables. RSTP category (six levels) was entered as a fixed effect, and participant ID was modeled as a random intercept to account for inter-individual variability. *Post hoc* analyses across the six RSTPs revealed distinct patterns of synchronization (i.e., increased FC) and desynchronization (i.e., reduced FC). Significant differences were observed across 18 of 21 between-network FC edges ($F_{(100,34340)} = 2.28$, $p < .0001$; Table 1) and 5 of 7 within-network core functional networks ($F_{(30,12026)} = 1.91$, $p = .002$, Table 2), based on a significance threshold of $\alpha = 0.05$. For each contrast, the unstandardized slope coefficient (*b*) was reported as an effect size, along with its 95% confidence interval. Tables 1 and 2 present the significant *post hoc* comparisons, including effect sizes (*b*), standard errors (SE), degrees of freedom (df), *t*-values, *p*-values, and confidence intervals (lower.CL and upper.CL), providing a detailed summary of the connectivity differences across RSTPs.

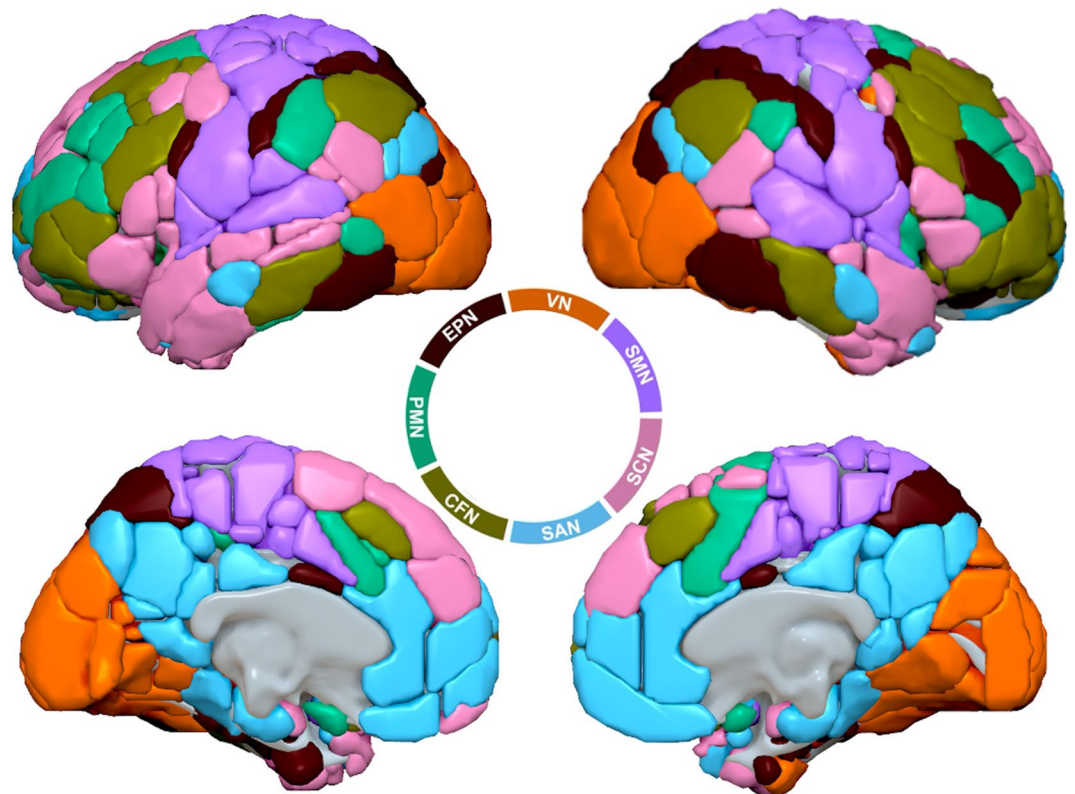


Fig. 1. The 3D brain mapping of the seven core functional networks. Social and communication network (SCN, including typically named LAN and social network): spoken language to monitor one's own speech and interpret the intentions, emotions, and beliefs of others during communication (pink). Self-awareness network (SAN, including typically named DMN and SN): enablers of individuals to use their internal resources - such as memory and self-awareness - to make decisions and behave by promoting reflective and independent thinking (blue). Cognitive flexibility network (CFN, typically named FPN): adaptation to changing circumstances and dynamically adjusting strategies to new information (khaki). Performance monitoring network (PMN, typically named CON): self-regulation and task performance improvement (green). Executive planning network (EPN, comparable to typically named and extended DAN): facilitation of adaptive behavior by enabling environment assessment, informed decisions, and effective goal-directed actions (brown). Somatomotor network (SMN): integration of sensory and motor functions, enabling movement, body awareness, and coordinated interaction with the surrounding environment (violet). Visual network (VN): perception, interpretation, and recognition of visual stimuli (orange).

Differential involvement of core functional networks across spontaneous thought profiles

To quantify the involvement of each core functional network in between-group FC differences, we computed a Differential Degree Count (DDC). For each of the seven nodes (networks), we counted the number of times it was involved in an edge that showed a statistically significant difference in between-network FC across the 15 pairwise comparisons between the six RSTP groups (21 possible edges). These differences were further classified as either synchronizations (increased FC in one RSTP relative to another) or desynchronizations (decreased FC). The DDC, inspired by *degree centrality*, thus reflects the total number of significant between-group differences involving a given node, allowing us to identify which core functional networks are more frequently involved in synchronizations or desynchronizations for each RSTP (Table 3).

We further observed a monotonic positive association between the proportion of between-network FC desynchronizations and the proportion of participants reporting high thought fluctuations, calculated at the RSTP level (*Spearman's* $\rho = 0.81$, $p = .049$; see Table 4).

The fluctuating profile, marked by the highest proportion of participants reporting high thought fluctuations (94%), was predominantly linked to desynchronizations, accounting for 88% of significant differences. In contrast, the verbal-predominant profile exhibited the lowest proportion of participants reporting high thought fluctuations (64%) and the lowest proportion of desynchronizations, representing only 12% of significant differences.

FC patterns characterizing spontaneous thought profiles

By comparing FC across the six RSTPs, we observed that the two evocative profiles shared a distinctive FC pattern, marked by: (i) SAN-VN integration distinguishing them from the two modality-predominant profiles, (ii) PMN-SMN integration distinguishing them from the vigilant and verbal-predominant profiles, and (iii)

Contrast	Edge	b	SE	df	Lower.CL	Upper.CL	t.value	p.value
RSTP 3 - RSTP 4	SCN_SAN	-0.0335	0.0128	32468.89	-0.0586	-0.0085	-2.62	0.0088
RSTP 3 - RSTP 5	SCN_SAN	-0.0238	0.0120	32468.89	-0.0474	-0.0002	-1.98	0.0477
RSTP 3 - RSTP 6	SCN_SAN	-0.0479	0.0190	32468.89	-0.0852	-0.0105	-2.51	0.0120
RSTP 2 - RSTP 3	SCN_CFN	0.0261	0.0112	32468.89	0.0042	0.0480	2.34	0.0193
RSTP 3 - RSTP 4	SCN_CFN	-0.0337	0.0128	32468.89	-0.0588	-0.0086	-2.63	0.0085
RSTP 3 - RSTP 5	SCN_CFN	-0.0249	0.0120	32468.89	-0.0485	-0.0013	-2.07	0.0384
RSTP 3 - RSTP 4	SCN_SMN	0.0337	0.0128	32468.89	0.0086	0.0588	2.63	0.0085
RSTP 3 - RSTP 5	SCN_SMN	0.0288	0.0120	32468.89	0.0052	0.0523	2.39	0.0167
RSTP 3 - RSTP 4	SAN_CFN	-0.0320	0.0128	32468.89	-0.0571	-0.0069	-2.50	0.0125
RSTP 3 - RSTP 5	SAN_CFN	-0.0236	0.0120	32468.89	-0.0472	-0.0001	-1.97	0.0493
RSTP 2 - RSTP 5	SAN_PMN	-0.0235	0.0112	32468.89	-0.0454	-0.0016	-2.10	0.0357
RSTP 4 - RSTP 5	SAN_PMN	-0.0272	0.0128	32468.89	-0.0523	-0.0021	-2.12	0.0338
RSTP 1 - RSTP 6	SAN_EPN	-0.0470	0.0214	32468.89	-0.0889	-0.0050	-2.19	0.0284
RSTP 2 - RSTP 6	SAN_EPN	-0.0462	0.0185	32468.89	-0.0824	-0.0099	-2.50	0.0126
RSTP 3 - RSTP 5	SAN_EPN	-0.0248	0.0120	32468.89	-0.0483	-0.0012	-2.06	0.0394
RSTP 3 - RSTP 6	SAN_EPN	-0.0580	0.0190	32468.89	-0.0953	-0.0206	-3.04	0.0023
RSTP 4 - RSTP 6	SAN_EPN	-0.0432	0.0195	32468.89	-0.0814	-0.0049	-2.21	0.0271
RSTP 1 - RSTP 5	SAN_VN	-0.0350	0.0155	32468.89	-0.0654	-0.0046	-2.26	0.0240
RSTP 1 - RSTP 6	SAN_VN	-0.0583	0.0214	32468.89	-0.1003	-0.0163	-2.72	0.0065
RSTP 2 - RSTP 6	SAN_VN	-0.0407	0.0185	32468.89	-0.0769	-0.0044	-2.20	0.0280
RSTP 3 - RSTP 5	SAN_VN	-0.0250	0.0120	32468.89	-0.0485	-0.0014	-2.08	0.0376
RSTP 3 - RSTP 6	SAN_VN	-0.0483	0.0190	32468.89	-0.0856	-0.0110	-2.54	0.0112
RSTP 4 - RSTP 6	SAN_VN	-0.0434	0.0195	32468.89	-0.0817	-0.0052	-2.22	0.0261
RSTP 2 - RSTP 4	SAN_SMN	0.0397	0.0120	32468.89	0.0162	0.0632	3.31	0.0009
RSTP 3 - RSTP 4	SAN_SMN	0.0454	0.0128	32468.89	0.0203	0.0705	3.55	0.0004
RSTP 4 - RSTP 6	SAN_SMN	-0.0595	0.0195	32468.89	-0.0978	-0.0212	-3.05	0.0023
RSTP 1 - RSTP 2	CFN_PMN	0.0344	0.0149	32468.89	0.0052	0.0635	2.31	0.0207
RSTP 1 - RSTP 6	CFN_PMN	0.0623	0.0214	32468.89	0.0203	0.1043	2.91	0.0036
RSTP 2 - RSTP 3	CFN_PMN	-0.0421	0.0112	32468.89	-0.0640	-0.0202	-3.77	0.0002
RSTP 3 - RSTP 4	CFN_PMN	0.0385	0.0128	32468.89	0.0134	0.0635	3.00	0.0027
RSTP 3 - RSTP 5	CFN_PMN	0.0364	0.0120	32468.89	0.0128	0.0599	3.02	0.0025
RSTP 3 - RSTP 6	CFN_PMN	0.0700	0.0190	32468.89	0.0327	0.1074	3.68	0.0002
RSTP 2 - RSTP 3	CFN_EPN	-0.0249	0.0112	32468.89	-0.0468	-0.0030	-2.23	0.0256
RSTP 2 - RSTP 4	CFN_EPN	-0.0389	0.0120	32468.89	-0.0624	-0.0154	-3.24	0.0012
RSTP 2 - RSTP 6	CFN_EPN	-0.0419	0.0185	32468.89	-0.0781	-0.0056	-2.26	0.0237
RSTP 1 - RSTP 4	CFN_VN	-0.0445	0.0161	32468.89	-0.0761	-0.0130	-2.77	0.0056
RSTP 1 - RSTP 6	CFN_VN	-0.0447	0.0214	32468.89	-0.0867	-0.0027	-2.09	0.0370
RSTP 2 - RSTP 4	CFN_VN	-0.0358	0.0120	32468.89	-0.0593	-0.0122	-2.98	0.0029
RSTP 2 - RSTP 3	CFN_SMN	-0.0225	0.0112	32468.89	-0.0444	-0.0006	-2.01	0.0440
RSTP 4 - RSTP 5	PMN_EPN	0.0294	0.0128	32468.89	0.0043	0.0545	2.29	0.0219
RSTP 2 - RSTP 4	PMN_VN	-0.0364	0.0120	32468.89	-0.0599	-0.0129	-3.04	0.0024
RSTP 2 - RSTP 5	PMN_VN	-0.0237	0.0112	32468.89	-0.0456	-0.0018	-2.12	0.0342
RSTP 1 - RSTP 4	PMN_SMN	-0.0439	0.0161	32468.89	-0.0754	-0.0123	-2.73	0.0064
RSTP 1 - RSTP 5	PMN_SMN	-0.0356	0.0155	32468.89	-0.0660	-0.0052	-2.29	0.0218
RSTP 1 - RSTP 6	PMN_SMN	-0.0485	0.0214	32468.89	-0.0905	-0.0065	-2.26	0.0235
RSTP 2 - RSTP 4	PMN_SMN	-0.0255	0.0120	32468.89	-0.0490	-0.0020	-2.13	0.0334
RSTP 3 - RSTP 4	PMN_SMN	-0.0459	0.0128	32468.89	-0.0710	-0.0208	-3.58	0.0003
RSTP 3 - RSTP 5	PMN_SMN	-0.0376	0.0120	32468.89	-0.0612	-0.0140	-3.13	0.0018
RSTP 3 - RSTP 6	PMN_SMN	-0.0505	0.0190	32468.89	-0.0879	-0.0132	-2.65	0.0080
RSTP 2 - RSTP 6	EPN_VN	-0.0386	0.0185	32468.89	-0.0749	-0.0024	-2.09	0.0368
Continued								

Contrast	Edge	b	SE	df	Lower.CL	Upper.CL	t.value	p.value
RSTP 1 - RSTP 3	EPN_SMN	0.0372	0.0155	32468.89	0.0069	0.0676	2.40	0.0163
RSTP 1 - RSTP 5	EPN_SMN	0.0401	0.0155	32468.89	0.0097	0.0705	2.59	0.0097
RSTP 1 - RSTP 4	VN_SMN	0.0387	0.0161	32468.89	0.0071	0.0702	2.40	0.0162
RSTP 2 - RSTP 3	VN_SMN	-0.0305	0.0112	32468.89	-0.0524	-0.0086	-2.73	0.0063
RSTP 3 - RSTP 4	VN_SMN	0.0471	0.0128	32468.89	0.0220	0.0722	3.68	0.0002

Table 1. Significant differences of between-network FC according to the RSTPs. *Note.* RSTP 1: evocative-preoccupied profile; RSTP 2: fluctuating profile; RSTP 3: evocative-reverie profile; RSTP 4: vigilant profile; RSTP 5: visual-predominant profile; RSTP 6: verbal-predominant profile.

Contrast	Network	b	SE	df	Lower.CL	Upper.CL	t.value	p.value
RSTP 1 - RSTP 2	PMN	0.0133	0.0066	12089.41	0.0004	0.0262	2.0265	0.0427
RSTP 2 - RSTP 3	PMN	-0.0123	0.0049	12089.41	-0.0220	-0.0026	-2.4933	0.0127
RSTP 2 - RSTP 3	SAN	0.0173	0.0049	12089.41	0.0077	0.0270	3.5146	0.0004
RSTP 3 - RSTP 4	SAN	-0.0205	0.0057	12089.41	-0.0316	-0.0094	-3.6242	0.0003
RSTP 3 - RSTP 5	SAN	-0.0117	0.0053	12089.41	-0.0221	-0.0013	-2.2067	0.0274
RSTP 3 - RSTP 6	SAN	-0.0256	0.0084	12089.41	-0.0421	-0.0091	-3.0441	0.0023
RSTP 2 - RSTP 6	SCN	0.0167	0.0082	12089.41	0.0007	0.0327	2.0452	0.0409
RSTP 5 - RSTP 6	SCN	0.0187	0.0084	12089.41	0.0022	0.0352	2.2200	0.0264
RSTP 2 - RSTP 4	SMN	0.0150	0.0053	12089.41	0.0046	0.0254	2.8274	0.0047
RSTP 2 - RSTP 5	SMN	0.0100	0.0049	12089.41	0.0003	0.0196	2.0178	0.0436
RSTP 2 - RSTP 6	SMN	0.0215	0.0082	12089.41	0.0055	0.0375	2.6323	0.0085
RSTP 3 - RSTP 4	SMN	0.0121	0.0057	12089.41	0.0010	0.0232	2.1412	0.0323
RSTP 3 - RSTP 6	SMN	0.0186	0.0084	12089.41	0.0021	0.0351	2.2147	0.0268
RSTP 1 - RSTP 5	VN	0.0138	0.0069	12089.41	0.0004	0.0272	2.0121	0.0442
RSTP 2 - RSTP 5	VN	0.0135	0.0049	12089.41	0.0038	0.0232	2.7297	0.0063
RSTP 3 - RSTP 5	VN	0.0107	0.0053	12089.41	0.0003	0.0212	2.0244	0.0430

Table 2. Significant differences of within-network FC according to the RSTPs. *Note.* RSTP 1: evocative-preoccupied profile; RSTP 2: fluctuating profile; RSTP 3: evocative-reverie profile; RSTP 4: vigilant profile; RSTP 5: visual-predominant profile; RSTP 6: verbal-predominant profile

CFN-PMN synchronization distinguishing them from the fluctuating and verbal-predominant profiles (Fig. 2). Additionally, we identified unique FC patterns, which reflected specific network configurations consistent with the qualitative content of spontaneous thoughts associated with each profile, as depicted in Fig. 3. The evocative-preoccupied profile was associated with CFN-VN integration, whereas the evocative-reverie profile was linked to CFN-SCN, CFN-SAN, SAN-SCN, and EPN-SAN integrations. The vigilant profile showed integration between the SMN and SAN, as well as between SMN and VN. The fluctuating profile was characterized by CFN-EPN and PMN-VN integrations. In contrast, the visual and verbal-predominant profiles were associated with the segregation of the VN and SCN, respectively.

Discussion

Using the GINNA atlas, we identified seven core functional networks whose degree of desynchronization was positively correlated with the richness of spontaneous thought dynamics across participants. FC comparisons across the six RSTPs revealed that the two evocative profiles shared a common FC pattern that reliably distinguished them from the others. In addition, each RSTP displayed distinct FC signatures that aligned with their respective thought content, highlighting differential engagement of large-scale brain networks in shaping spontaneous mental activity.

We observed a consistent association between reduced FC and spontaneous thought profiles, suggesting that greater network involvement in mental content is accompanied by lower synchronization, both within and between core functional networks. These results align with studies emphasizing a dissociation between neural activation and functional connectivity^{53,61-63}, supporting the notion that cognitive engagement can reduce FC rather than increase it. Furthermore, our results are consistent with the observation that high neural activity often coincides with lower FC in the resting brain⁵². Our findings reinforce theoretical models of FC dynamics, which propose that high connectivity may correspond to a resting or standby state, while desynchronization may indicate active, task-like processing⁵⁷⁻⁵⁹. In this view, decreased FC reflect network dynamic recruitment in spontaneous cognitive operations.

The two evocative spontaneous thought profiles represent rich and diverse mental states characterized by internally oriented, self-referential, and empathic thoughts, accompanied by vivid imagery and emotionally

Thought profile	SCN	SAN	CFN	PMN	EPN	VN	SMN	Total
Desynchronization								
Evocative-preoccupied	-	3	2	3	1	4	3	16
Fluctuating	-	3	7	6	5	6	3	30
Evocative-reverie	6	9	5	3	3	2	4	32
Vigilant	1	7	1	2	1	3	7	22
Visual-predominant	1	-	1	2	2	-	2	8
Verbal-predominant	-	-	2	2	-	-	-	4
Total	8	22	18	18	12	15	19	
Synchronization								
Evocative-preoccupied	-	-	2	2	2	1	3	10
Fluctuating	1	1	1	-	-	-	1	4
Evocative-reverie	2	1	6	4	1	2	6	22
Vigilant	2	2	5	5	2	3	3	22
Visual-predominant	2	8	2	5	1	3	3	24
Verbal-predominant	1	10	2	2	6	6	3	30
Total	8	22	18	18	12	15	19	

Table 3. Differential degree count (DDC) by core functional network and thought profile. *Note.* Each cell reports the number of significant between-network FC differences involving the corresponding core functional network for each RSTP, based on 15 pairwise comparisons. Synchronizations and desynchronizations are both included in this count, reflecting each network's involvement in RSTP-specific FC variation

Variable / Profile	Evocative-preoccupied	Fluctuating	Evocative-reverie	Vigilant	Visual-predominant	Verbal-predominant
Désynchronisations (% DDC)	61	88	59	50	25	12
High Thought Fluctuations (% Participants)	87	94	87	90	86	64

Table 4. Correlation between the proportion of between-network FC desynchronizations and the proportion of participants reporting high thought fluctuations across the six RSTPs. *Note.* A desynchronization is defined as a significant edge FC decrease in one RSTP relative to another. For each RSTP, the proportion of desynchronizations was calculated by dividing the number of desynchronized nodes by the total number of nodes involved in significant between-network FC differences. High thought fluctuation corresponds to the proportion of participants within each RSTP reporting more than three concurrent thought themes. Data on thought fluctuation thresholds previously published in ⁴⁷.

salient recollections or imaginative scenes. These profiles were associated with common patterns of FC, which contrasted with those observed in other profiles along three main dimensions (Fig. 2).

First, SAN-VN desynchronization was observed in the two evocative profiles, contrasting with synchronization in the two modality-predominant profiles (visual-predominant and verbal-predominant). This synchronization in the latter may reflect the relative paucity of their thought content: the visual-predominant profile was marked by sparse mental content, while the verbal-predominant profile primarily centers on surroundings and cardiorespiratory awareness. The involvement of the SAN in the evocative profiles is consistent with prior evidence linking the DMN to self-referential processing, social cognition, and autobiographical memory²⁵ (e.g., vivid internal experiences during working memory maintenance⁶⁴, and perspective-taking or simulation of others' experiences⁶⁵). Furthermore, SAN-VN integration has been associated with mental imagery^{66,67}, creativity⁶⁸, and heightened vividness linked to early visual cortex activation⁶⁹. In this context, SAN-VN coupling may contribute to the vividness and creativity in the evocative profiles.

Second, CFN-PMN synchronization in the evocative profiles contrasted with desynchronization in the fluctuating and verbal-predominant profiles. These latter two are defined by alternating internal and external attention, and their CFN-PMN integration likely supports this cognitive flexibility and attentional reorientation, consistent with their known roles in task switching and attentional control^{25,30,70}.

Third, PMN-SMN desynchronization in the evocative profiles contrasted with PMN-SMN synchronization in the vigilant and modality-predominant profiles. The evocative profiles were also associated with reduced movement during scanning, unlike the verbal-predominant and vigilant profiles, which showed greater in-scanner motion. Additionally, within-network SMN desynchronization was observed in the vigilant and verbal-predominant profiles, possibly reflecting increased sensorimotor engagement due to higher mobility. Conversely, PMN-SMN integration in the evocative profiles may reflect efficient motor suppression or stabilized motor control, facilitating the internally immersive experience. This interpretation aligns with the PMN's proposed

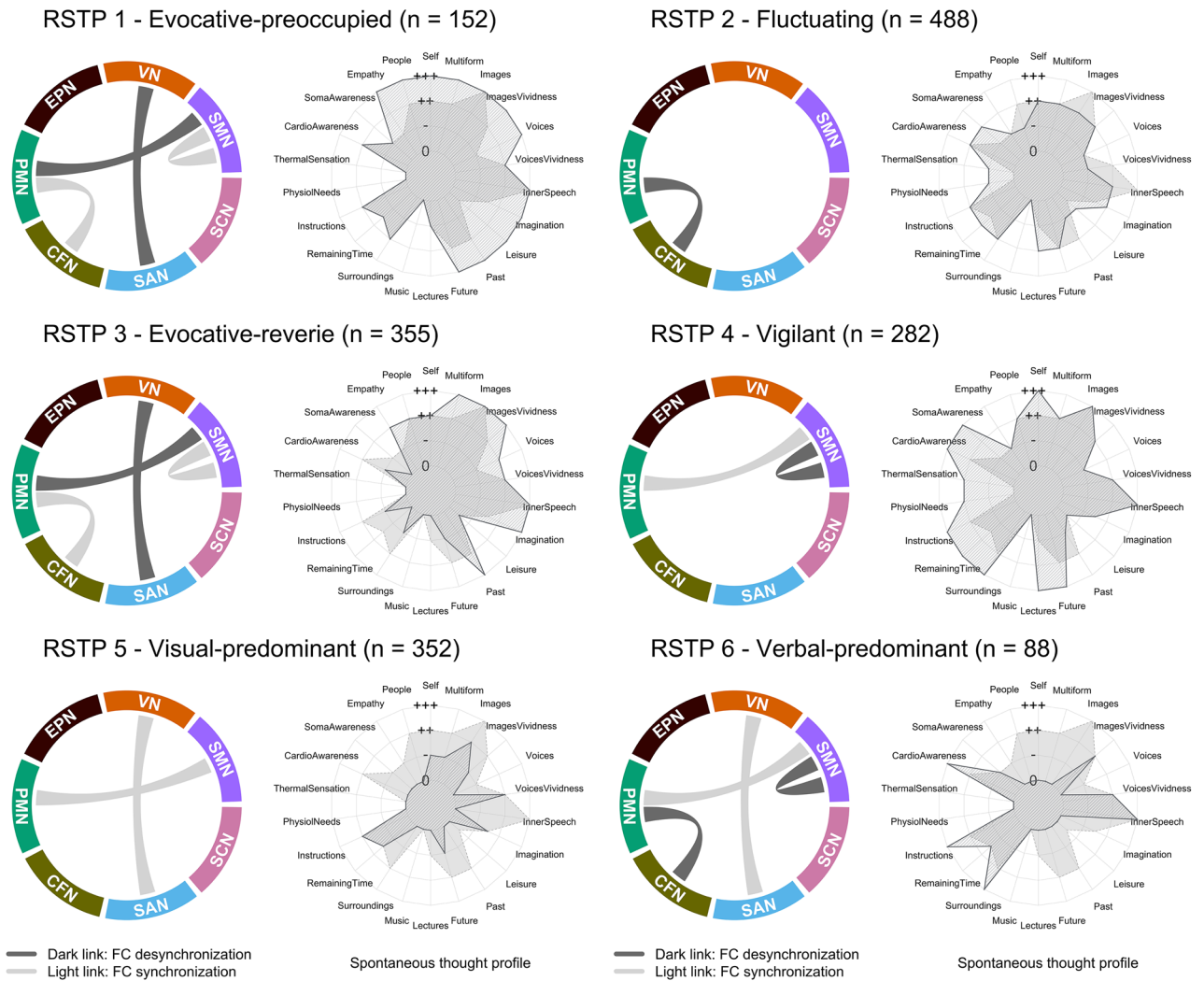


Fig. 2. FC Patterns associated with several RSTPs. Chord diagrams show FC variations associated with at least two RSTPs. Links indicate a significant difference for the RSTP compared to at least two others. Dark grey links indicate significant desynchronization (i.e., decreased FC). Light grey links indicate significant synchronization (i.e., increased FC). Radar plots show RSTP characterization by the ReSQ 2.0 categories ($N = 1779$). The background gray profile represents the most frequent categories in the study sample. 0 = never, - = rarely, + + = often, + + + = very often, except for voice vividness: - = rather vague, + + = rather precise and image vividness: - = few details, + + = moderate details, + + + = many details. Detailed characterization was displayed in⁴⁷.

role in maintaining stable implementation of task sets in downstream sensorimotor processors across trials³⁰ and its FC with the SMN^{26,71}.

In addition to the shared features, distinct FC patterns were also observed for specific thought profiles, indicating that each profile engages partially dissociable network dynamics (Fig. 3).

The evocative-reverie profile was specifically linked to an extensive integration of functional core networks, including the CFN, EPN, SAN, and SCN. Empathic, past-oriented, and imaginative thoughts of the evocative-reverie profile align with previous research linking CFN-SAN interaction to creative thinking⁷²⁻⁷⁵ and temporally extended evaluation of self-generated thoughts⁷⁶. The specific involvement of the SCN, encompassing regions such as the anterior temporoparietal junction, inferior frontal gyrus, and posterior middle temporal gyrus, known for their roles in processing language and depictions of human behavior⁶⁵, suggests that the evocative-reverie profile engaged in mentalizing social scenes through an allocentric perspective. Consistently, several authors emphasize that allocentric representations require broad inter-network interactions to support their complexity^{77,78}. The integration between the SAN and EPN (an extended version of the DAN) might have seemed intriguing, given the frequently documented anticorrelation between the SAN and EPN. However, Dixon et al.⁷⁹ have shown that SAN-EPN FC fluctuates over time and contexts, coordinated by broader network dynamics involving the CFN, a tripartite interaction also observed in the evocative-reverie profile. Notably, they observed that the frontal eye fields (part of the EPN) and the dorsomedial prefrontal cortex (part of the SAN) exhibited stronger negative FC during a movie-watching condition compared to rest. The similarity between their findings and ours supports that the evocative-reverie profile favored an outward-focused perspective.

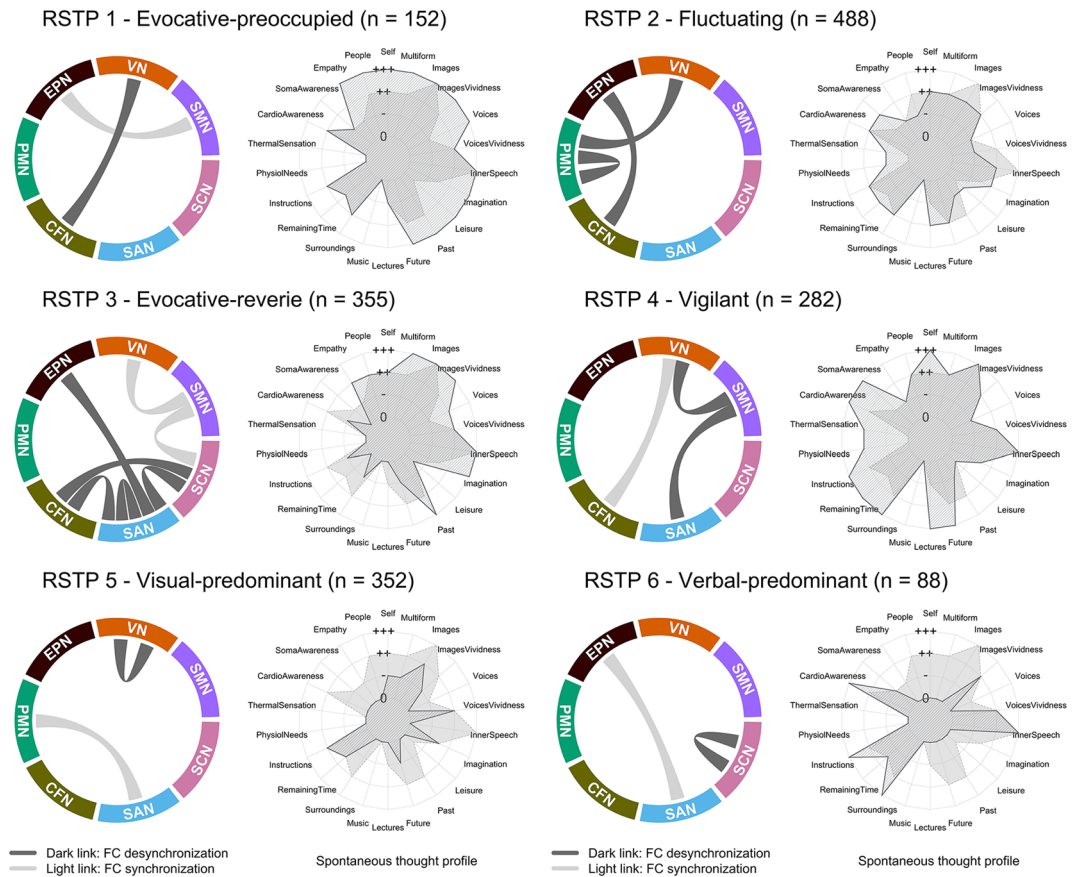


Fig. 3. FC Patterns specifically associated with each RSTP. Chord diagrams show FC variations associated with each RSTP. Links indicate a significant difference for the RSTP compared to at least two others. Dark grey links indicate significant desynchronization (i.e., decreased FC). Light grey links indicate significant synchronization (i.e., increased FC). Radar plots show RSTP characterization by the ReSQ 2.0 categories ($N = 1779$). The background gray profile represents the most frequent categories in the study sample. 0 = never, - = rarely, ++ = often, +++ = very often, except for voice vividness: - = rather vague, ++ = rather precise and image vividness: - = few details, ++ = moderate details, +++ = many details. Detailed characterization was displayed in⁴⁷.

Within SAN-EPN integration, it is plausible that EPN involvement facilitated flexibility in supporting allocentric spatial representations⁸⁰.

In contrast to the evocative-reverie profile, the high co-occurrence of self-referential and empathic thoughts in the evocative-preoccupied profile strongly aligns it with a first-person perspective^{81,82}. Accordingly, the evocative-preoccupied profile exhibited limited specific functional integration, involving only the CFN-VN. We hypothesize that the evocative-preoccupied profile adopted an egocentric perspective in which individuals “see” themselves within the scene, engaging visual simulation processes analogous to those activated during real-world perception⁸³ while requiring significantly less functional integration than the allocentric perspective of the evocative-reverie profile. In support of this hypothesis, CFN-VN integration is associated with mental imagery process⁶⁷, with the CFN contributing to subjective vividness and the VN enhancing its precision^{84,85}.

The fluctuating profile is a diverse profile mixing internally and externally oriented thoughts and was characterized by the highest level of thought fluctuations (Table 4). The fluctuating profile was associated with a specific FC pattern integrating CFN-EPN and PMN-VN. This finding is consistent with previous literature showing that executive function networks likely work as an ensemble to produce accurate and timely individual switching behaviors⁸⁶.

The vigilant profile is focused on externally and bodily-oriented thoughts and was linked to the integration of SMN-VN and SAN-SMN. SAN-SMN integration was previously linked to low-level frequency daydreaming⁸⁷ and observed in task-focused trials compared to stimulus-independent, task-unrelated thought⁸⁸. The prominent involvement and integration of the SAN and SMN in the vigilant profile (Table 3) likely underpin the heightened experience of painful and unpleasant sensations previously associated with this profile⁴⁷. These findings suggest that the SAN (comprising the DMN and SN) may play a pivotal role in modulating integrated self-consciousness by linking external stimuli to interoception and nociception.

The visual-predominant thoughts are distinguished by their exclusive use of images, whereas the verbal-predominant thoughts rely solely on inner speech. Accordingly, the visual-predominant profile was associated with VN segregation, and the verbal-predominant profile with SCN segregation, both without any connection

to a specific integration pattern. These sparse and modality-predominant profiles were the only ones linked to FC segregation, underscoring the unique relationship between cognitive modes and functional network organization.

Conclusion

We present a comprehensive and integrated framework for understanding the dynamics of core functional network integration and segregation in relation to spontaneous thought profiles during rfMRI scans. Our findings reveal that the sparsest thought profiles are characterized by pronounced segregation of core networks, aligning with specific cognitive modes. In contrast, rich and diverse thought profiles exhibit distinct patterns of functional integration consistent with the established roles of the brain regions forming these networks. These results support a broader conceptualization of the ‘default mode,’ extending beyond the narrow confines of the DMN to encompass dynamic and distributed brain activity. We propose that the resting-state reflects a personalized integration of core functional networks, producing distinct FC patterns. By modeling inter-individual variability across six well-characterized thought profiles, we demonstrate that this process underpins unique cognitive and introspective functions.

Methods

Participants

We leveraged data from the MRi-Share project, a large-scale prospective cohort of French university students, to explore neuroanatomical maturation and variability in healthy young adults⁸⁹. From the 1,870 MRi-Share participants, native French speakers with usable MRI data were included, alongside those who completed the ReSQ 2.0, a tool for evaluating the quality and content of thoughts during resting-state periods, resulting in a final sample of 1,717 individuals (mean age 22 ± 2.25 years, 72% women). All procedures were performed in compliance with the declaration of Helsinki and were approved by the Comité de Protection des Personnes Sud-Ouest et Outre-Mer (local ethics committee CPP SOOMIII) with agreement 2015-A00850-49. All participants signed an informed written consent form.

Resting-state spontaneous thoughts assessment

The ReSQ 2.0 (24-item self-report) evaluates spontaneous mental activity at rest⁴⁷. To classify individuals into homogeneous thought subgroups, we applied agglomerative hierarchical clustering with Ward’s method and Euclidean distances based on multiple correspondence analysis components, followed by K-means clustering for refinement. This analysis identified six distinct resting-state thought profiles (RSTPs), summarized below:

- An *evocative-preoccupied* profile: A profile focused on internally oriented thoughts, self-relevant preoccupations, thoughts about others with empathy, past events, and future thinking, with precise images and voices and negative emotional valence (RSTP 1, $n = 152$).
- A *fluctuating* profile: The most fluctuating profile, with diverse thoughts alternating between externally and internally oriented thoughts, is close to the average profile of all participants (RSTP 2, $n = 488$).
- An *evocative-reverie* profile: A profile exclusively involving internally oriented thoughts about others with empathy, past events, and imaginative scenes, with precise images and voices and positive emotional valence (RSTP 3, $n = 355$).
- A *vigilant* profile: A profile centered on externally and bodily-oriented thoughts, future thinking, and lectures, with a negative emotional valence (RSTP 4, $n = 282$).
- A *visual-predominant* profile: The least defined profile, with exclusive use of images (RSTP 5, $n = 352$).
- A *verbal-predominant* profile: The least fluctuating profile, concentrating on surroundings and cardiorespiratory awareness, exclusively using inner speech (RSTP 6, $n = 88$).

Additionally, analysis of the quality control metric for head motion (mean absolute translation⁶⁷) revealed that the two internally-oriented evocative profiles were associated with significantly less movement compared to the vigilant and verbal-predominant profiles (RSTP 1 vs.4: $b = -0.0126$, $t = -2.29$, $p = .022$; RSTP 1 vs. 6: $b = -0.0172$, $t = -2.36$, $p = .018$; RSTP 3 vs.4: $b = -0.0113$, $t = -2.6$, $p = .009$; RSTP 3 vs.6: $b = 0.016$, $t = 2.46$, $p = .014$).

FC analyses and core functional networks delineation

One thousand seven hundred seventeen participants completed a 15-minute rfMRI scan with closed eyes. Data acquisition and preprocessing details can be found elsewhere⁸⁹. FC was computed using the GINNA atlas¹⁸ and is available for download at <https://github.com/Achillegillig/ginna>. The non-overlapping version of this atlas includes 439 brain regions, each assigned to one of 33 functional networks and classified into one of three tissue types: Cortex, Basal Ganglia, or Cerebellum. For the present analysis, only cortical regions were included, resulting in a decomposition into 32 networks (one exclusively covers basal ganglia regions) with a minimum of 2 and a maximum of 17 regions per network.

Core functional networks were identified through a hierarchical ascending classification of the 32 networks, following the method outlined in Doucet et al.¹³. The average time course of voxels within each GINNA atlas region was computed. The time course of each functional network was calculated as the average of the time courses of its constituent regions. FC values between the 32 networks were quantified as the Fisher z -transformed Pearson correlation coefficients between the time courses of any two functional networks. Then, FC values were averaged across participants, and hierarchical clustering was implemented using the average-linkage method. Correlation values were converted into dissimilarity distances and aggregated based on minimal dissimilarity. Clustering reliability was assessed using the *pvclust* R package, employing a bootstrap resampling approach on

Cluster	Cognitive Label	GINNA's Cognitive Correspondences	Anatomical Label	Main Cortical Areas
C01	Social and Communication Network (SCN)	Speech perception Syntactic processing Sentence comprehension Self-monitoring Theory of mind	Ventral frontoparietal network (V-FPN)	Anterior temporal lobe Anterior temporoparietal junction (posterior superior temporal sulcus, ventral posterior supramarginal gyrus) Dorsomedial prefrontal cortex Inferior frontal gyrus (pars triangularis, pars orbitalis Left) Middle precentral sulcus Left Superior frontal gyrus Superior temporal gyrus Supplementary motor area
C02	Self-Awareness Network (SAN)	Decision making Memory retrieval Self-referential processing	Medial frontoparietal network (M-FPN)	Anterior cingulate cortex Dorsal frontal lobe Medial temporal lobe (Hippocampus, Parahippocampal cortex) Middle temporal gyrus Parieto-occipital sulcus Posterior cingulate cortex Posterior inferior parietal lobule Posterior temporoparietal junction (caudal angular gyrus) Ventral anterior insula Ventral precuneus Ventromedial prefrontal cortex
C03	Cognitive Flexibility Network (CFN)	Interference resolution Phonological working memory Reasoning	Lateral frontoparietal network (L-FPN)	Dorsal inferior parietal lobule - Left Inferior temporal lobe Middle and inferior frontal lobe Pre-Supplementary Motor Area Rostral angular gyrus
C04	Performance Monitoring Network (PMN)	Expectancy Performance monitoring Working memory	Midcingulo-insular network (M-CIN)	Anterior midcingulate cortex Dorsal anterior insula Middle and superior frontal lobe Dorsal posterior supramarginal gyrus
C05	Executive Planning Network (EPN)	Mental arithmetic Motor planning Reading Spatial selective attention	Dorsal frontoparietal network (D-FPN)	Dorsal anterior precuneus Dorsal anterior supramarginal gyrus Frontal Eye Fields Lateral fusiform gyrus - Left Lateral orbitofrontal cortex - Right Middle frontal lobe - Right Posterior inferotemporal area Posterior superior parietal lobule and intraparietal sulcus
C06	Visual Network (VN)	Object perception Motion detection Visual form discrimination Visual object recognition Visual perception	Occipital network (ON)	Occipital lobe Parietoccipital Sulcus Posterior fusiform gyrus
C07	SomatoMotor Network (SMN)	Articulation Auditory perception Movement (limb, right and left hand) Motor imagery Somatosensation	Pericentral network (PN)	Central regions (paracentral lobule, Rolandic operculum, central sulcus, precentral and dorsal postcentral sulcus) Mid-posterior cingulate sulcus Mid-posterior insula Superior anterior parietal lobe Superior temporal gyrus Ventral supramarginal gyrus

Table 5. The anatomical and cognitive profiling of seven core functional networks.

100,000 datasets, ranging from 50 to 140% of the sample size⁹⁰. This analysis identified seven core functional networks, including 33 to 69 regions each.

Within-network FC of core functional networks was calculated as the average Pearson correlation coefficient (Fisher z-transformed) between the time courses of all region pairs within a single core functional network.

Between-network FC of core functional networks was defined in the same manner as for the GINNA atlas (see above).

The average Pearson correlation coefficient (Fisher z-transformed) across all region pairs (APCC) was calculated to estimate the drowsiness effects³⁸.

Anatomical and cognitive profiling of seven core functional networks

The anatomical organization of seven core functional networks is visualized in 3D in Fig. 1. Each network was assigned a synthesized cognitive label based on the corresponding cognitive functions described in the GINNA atlas¹⁸, independent of its anatomical description (Table 5).

The *Social and Communication Network* (SCN) clusters frontoparietal regions previously associated with language⁹¹ and dynamic representations of social interactions⁶⁵. The SCN includes social-related areas like the dorsomedial prefrontal cortex^{92,93}; semantic-associated areas, such as the superior frontal gyrus⁹⁴; and regions associated with both functions, including the left inferior frontal gyrus (pars triangularis and pars orbitalis left), anterior temporal lobe, supplementary motor area, superior temporal gyrus, and temporoparietal junction^{94–99}. The association between language and social networks is sometimes observed at rest^{94,100} and emerges from Kong's meta-analysis of eight FC atlases²⁰.

The *Self-Awareness Network* (SAN) outlines a medial frontoparietal network. It includes regions commonly identified in the literature as the DMN, specifically the posterior cingulate cortex, ventral precuneus, medial prefrontal cortex, medial temporal lobe (i.e., hippocampus and parahippocampal cortex), medial orbitofrontal cortex, caudal angular gyrus, posterior inferior parietal lobule, and parieto-occipital sulcus^{21,101,102}. The SAN also encompasses the SN, including the ventral anterior insula and rostral anterior cingulate cortex¹⁴. The DMN is an integrated system for autobiographical and semantic memory, self-monitoring, and empathic processing^{25,65}. The SN is a hub for consciously integrating autonomic feedback and responses with internal goals and external demands²⁸. The ventral anterior insula plays a central role in interoceptive awareness¹⁰³, body movement awareness, and self-recognition¹⁰⁴. It supports homeostatic demands²⁸ and emotional awareness^{104,105} in conjunction with the anterior cingulate. Thus, the SAN may support a context-sensitive self, integrating the introspective capacities of the DMN with the situational awareness and emotional relevance provided by the SN. Note that this SN is distinct from the one described by Menon et al.²⁵ which is more closely associated with the PMN. By uniting essential components of self-related processing and emotional experience, the SAN presents a system of *integrated self-consciousness* in line with the ‘sense of self’ concept attributed to the DMN²⁵.

Three networks represent the executive functions. First, the *Cognitive Flexibility Network* (CFN) includes portions of the lateral prefrontal cortex and posterior parietal cortex, e.g., the middle and inferior frontal lobe, pre-supplementary motor area, rostral angular gyrus, left inferior parietal lobule, and a portion of the inferior temporal lobe. The CFN is, therefore, a lateral frontoparietal network aligned with the well-described FPN^{23,30,34}. This similarity further reinforces the role of the CPN as a flexible hub for cognitive control³⁰. Second, the *Performance Monitoring Network* (PMN) comprises the dorsal anterior insula and anterior midcingulate cortex (i.e., the dorsal anterior cingulate cortex), along with regions of the middle and superior frontal lobe and the dorsal posterior supramarginal gyrus³⁷. The PMN is a midcingulo-insular network closely resembling the CON, which Dosenbach et al. renamed the action-mode network¹⁰⁶, aligning with its role in postural¹⁰⁷ and motor control³⁷. Third, the *Executive Planning Network* (EPN) incorporates core regions of the DAN, including the frontal eye fields, superior posterior parietal lobule, and intraparietal sulcus¹⁰⁸. The EPN encompasses additional regions, most of which had been previously associated with the DAN, such as the dorsal anterior precuneus¹⁰⁹, dorsal anterior supramarginal gyrus⁹⁸, posterior inferotemporal area^{108,110,111}, left lateral fusiform gyrus¹¹², right middle frontal lobe^{108,113}, and right lateral orbitofrontal cortex. The EPN broadens the DAN’s framework (i.e., visuospatial attention) by integrating regions tied to critical aspects of executive planning, encompassing high-level visual processing, like categorical recognition, and priority mapping, alongside evaluating potential outcomes and the sequencing of movements^{112,114–116}.

Classically, the SMN is a pericentral network encompassing the superior temporal gyrus, mid-posterior insula, superior anterior parietal lobe, and central regions such as Rolandic operculum, precentral, postcentral, and central sulcus. Also typical, the VN is located in the occipital lobe²¹.

Statistical analysis

Associations of spontaneous thoughts with variations in FC

To investigate how spontaneous thoughts relate to the integration and segregation of core functional networks, we analyzed between-network and within-network FC in relation to the RSTPs using two separate mixed linear regression models. Between-network FC (21 edges, calculated as $7 \times 6 \div 2$) and within-network FC were determined using Fisher’s *r*-to-*z* transformed correlation values and served as the outcomes. The RSTP category (6 levels) was included as the predictor, with participant ID specified as a random effect.

Estimation and hypothesis testing of coefficients

A resampling bootstrap method was used with 1,000-fold replication to evaluate the uncertainty about fixed effect coefficient estimates and validate the internal reliability of the effects¹¹⁷. This method showed good consistency among fixed effect coefficient estimates. Then, the significance of fixed effects was assessed using ANOVA components and residuals were visually inspected for normality and homoscedasticity.

Addressing the influence of confounding factors

Fixed-effect covariates, including total intracranial volume, age, gender/sex, and drowsiness (i.e., APCC), were incorporated into the mixed linear regression models to account for their potentially confounding effects^{38,118}.

Comparison of FC across the six RSTPs and interpretation threshold

To compare the FC of the six RSTPs, *post hoc* analyses were conducted using an alpha level of 0.05 for the significance threshold of hypothesis tests. The unstandardized slope coefficient (*b*) with its confidence interval was reported as effect size¹¹⁹. Detailed *post hoc* results, including effect sizes (*b*), standard errors (SE), degrees of freedom (df), *t*-values, *p*-values, and confidence intervals (lower.CL and upper.CL), are provided in Tables 1 and 2. Aiming to ensure the consistency of the observed differences, we focused exclusively on those involving one RSTP relative to at least two others to visualize and interpret the results.

Statistical analyses comparing RSTPs were conducted using RStudio (R 4.0.0)^{120,121}. Mixed linear regression models were fitted with the lmerTest package (version 3.1-3)¹²² and *post hoc* analyses were performed with the emmeans package (version 1.4.7)¹²³.

Data availability

The raw data are not publicly available due to restrictions on informed consent. The raw data supporting this study’s findings are available on request from the i-Share Scientific Collaborations Coordinator using the procedure described on the i-Share web site: <https://research.i-share.fr/>.

Received: 29 January 2025; Accepted: 3 July 2025

Published online: 04 August 2025

References

- Bassett, D. S. & Sporns, O. Network neuroscience. *Nat. Neurosci.* **20**, 353–364 (2017). <https://doi.org/10.1038/nn.4502>
- Thiebaut de Schotten, M. & Forkel, S. J. The emergent properties of the connected brain. *Science* **378**, 505–510 (2022). <https://doi.org/10.1126/science.abq2591>
- Snyder, A. Z. & Raichle, M. E. A brief history of the resting state: the Washington University perspective. *NeuroImage* **62**, 902–910 (2012). <https://doi.org/10.1016/j.neuroimage.2012.01.044>
- Mazoyer, B. et al. Cortical networks for working memory and executive functions sustain the conscious resting state in man. *Brain Res. Bull.* **54**, 287–298 (2001).
- Raichle, M. E. et al. A default mode of brain function. *Proc. Natl. Acad. Sci. USA* **98**, 676–682. <https://doi.org/10.1073/pnas.98.2.676> (2001).
- Cole, M. W. et al. Intrinsic and task-evoked network architectures of the human brain. *Neuron* **83**, 238–251. <https://doi.org/10.1016/j.neuron.2014.05.014> (2014).
- Salvo, J. J., Holubecki, A. M. & Braga, R. M. Correspondence between functional connectivity and task-related activity patterns within the individual. *Curr. Opin. Behav. Sci.* **40**, 178–188 (2021). <https://doi.org/10.1016/j.cobeha.2021.05.003>
- Smith, S. M. et al. Correspondence of the brain's functional architecture during activation and rest. *Proc Natl Acad Sci USA* **106**, 13040–13045 (2009). <https://doi.org/10.1073/pnas.0905267106>
- Laird, A. R. et al. Behavioral interpretations of intrinsic connectivity networks. *J. Cogn. Neurosci.* **23**, 4022–4037 (2011). https://doi.org/10.1162/jocn_a_00077
- Chenot, Q. et al. Functional connectivity within the fronto-parietal network predicts complex task performance: A fNIRS study. *Front. Neuroergonomics* **2**, 718176 (2021). <https://doi.org/10.3389/fnrgo.2021.718176>
- Liégeois, R. et al. Resting brain dynamics at different timescales capture distinct aspects of human behavior. *Nat. Commun.* **10**, 2317 (2019). <https://doi.org/10.1038/s41467-019-10317-7>
- Tavor, I. et al. Task-free MRI predicts individual differences in brain activity during task performance. *Science* **352**, 216–220 (2016). <https://doi.org/10.1126/science.aad8127>
- Doucet, G. et al. Brain activity at rest: a multiscale hierarchical functional organization. *J. Neurophysiol.* **105**, 2753–2763. <https://doi.org/10.1152/jn.00895.2010> (2011).
- Gordon, E. M. et al. Precision functional mapping of individual human brains. *Neuron* **95**, 791–807e7. <https://doi.org/10.1016/j.neuron.2017.07.011> (2017).
- Nozais, V. et al. Atlasing white matter and grey matter joint contributions to resting-state networks in the human brain. *Commun. Biol.* **6**, 726. <https://doi.org/10.1038/s42003-023-05107-3> (2023).
- Yeo, B. T. et al. The organization of the human cerebral cortex estimated by intrinsic functional connectivity. *J. Neurophysiol.* **106**, 1125–1165. <https://doi.org/10.1152/jn.00338.2011> (2011).
- Doucet, G., Lee, W. H. & Frangou, S. Evaluation of the spatial variability in the major resting-state networks across human brain functional atlases. *Hum. Brain. Mapp.* **40**, 4577–4587. <https://doi.org/10.1002/hbm.24722> (2019).
- Gillig, A. et al. GINNA, a 33 resting-state networks atlas with meta-analytic decoding-based cognitive characterization. *Commun. Biol.* **8**(1), 253. <https://doi.org/10.1038/s42003-025-07671-2> (2025).
- Hermosillo, R. J. M. et al. A precision functional atlas of personalized network topography and probabilities. *Nat. Neurosci.* **27**, 1000–1013. <https://doi.org/10.1038/s41593-024-01596-5> (2024).
- Kong, R. Q. et al. A network correspondence toolbox for quantitative evaluation of novel neuroimaging results. *Nat. Commun.* **16**(1), 2930. <https://doi.org/10.1038/s41467-025-58176-9> (2025).
- Uddin, L. Q., Yeo, B. T. T. & Spreng, R. N. Towards a universal taxonomy of macro-scale functional human brain networks. *Brain Topogr* **32**, 926–942. <https://doi.org/10.1007/s10548-019-00744-6> (2019).
- Uddin, L. Q. et al. Controversies and progress on standardization of large-scale brain network nomenclature. *Netw. Neurosci.* **7**, 864–905. https://doi.org/10.1162/netn_a_00323 (2023).
- Power, J. D. et al. Functional network organization of the human brain. *Neuron* **72**, 665–678. <https://doi.org/10.1016/j.neuron.2011.09.006> (2011).
- Rosazza, C. & Minati, L. Resting-state brain networks: Literature review and clinical applications. *Neurol. Sci.* **32**, 773–785. <https://doi.org/10.1007/s10072-011-0636-y> (2011).
- Menon, V. 20 years of the default mode network: A review and synthesis. *Neuron* **111**, 2469–2487. <https://doi.org/10.1016/j.neuron.2023.04.023> (2023).
- Gratton, C., Ladwig, Z. & Perez, D. C. What do network approaches add to our understanding of prefrontal cortex and executive function? in *The frontal cortex* (eds. Banich, M. T., Haber, S. N. & Robbins, T. W.) 203–224 (The MIT Press, 2024). <https://doi.org/10.7551/mitpress/15679.003.0014>
- Witt, S. T. et al. What executive function network is that? An image-based meta-analysis of network labels. *Brain Topogr* **34**, 598–607. <https://doi.org/10.1007/s10548-021-00847-z> (2021).
- Seeley, W. W. The salience network: A neural system for perceiving and responding to homeostatic demands. *J. Neurosci.* **39**, 9878–9882. <https://doi.org/10.1523/JNEUROSCI.1138-17.2019> (2019).
- Cole, M. W. et al. Multi-task connectivity reveals flexible hubs for adaptive task control. *Nat. Neurosci.* **16**, 1348–1355. <https://doi.org/10.1038/nn.3470> (2013).
- Marek, S. & Dosenbach, N. U. F. The frontoparietal network: function, electrophysiology, and importance of individual precision mapping. *Dialog. Clin. Neurosci.* **20**, 133–140. <https://doi.org/10.31887/DCNS.2018.20.2.smarek> (2018).
- Fox, M. D. et al. Spontaneous neuronal activity distinguishes human dorsal and ventral attention systems. *Proc. Natl. Acad. Sci. U.S.A.* **103**, 10046–10051. <https://doi.org/10.1073/pnas.0604187103> (2006).
- Szczepanski, S. M. et al. Functional and structural architecture of the human dorsal frontoparietal attention network. *Proc. Natl. Acad. Sci. U.S.A.* **110**, 15806–15811. <https://doi.org/10.1073/pnas.1313903110> (2013).
- D'Andrea, C. B. et al. Thalamo-cortical and cerebello-cortical functional connectivity in development. *Cereb. Cortex* **33**(15), 9250–9262. <https://doi.org/10.1093/cercor/bhad198> (2023).
- Ji, J. L. et al. Mapping the human brain's cortical-subcortical functional network organization. *NeuroImage* **185**, 35–57. <https://doi.org/10.1016/j.neuroimage.2018.10.006> (2019).
- Tomasi, D. & Volkow, N. D. Resting functional connectivity of language networks: characterization and reproducibility. *Mol. Psychiatry* **17**, 841–854. <https://doi.org/10.1038/mp.2011.177> (2012).
- Zhu, L. et al. Temporal reliability and lateralization of the resting-state Language network. *PLoS ONE* **9**, e85880. <https://doi.org/10.1371/journal.pone.0085880> (2014).
- Dosenbach, N. U. F. et al. Distinct brain networks for adaptive and stable task control in humans. *Proc. Natl. Acad. Sci. U.S.A.* **104**, 11073–11078. <https://doi.org/10.1073/pnas.0704320104> (2007).
- Joliot, M. et al. Modulate the impact of the drowsiness on the resting state functional connectivity. *Sci. Rep.* **14**, 8652. <https://doi.org/10.1038/s41598-024-59476-8> (2024).

39. Bolt, T. et al. Widespread autonomic physiological coupling across the brain-body axis. *Preprint At* <https://doi.org/10.1101/2023.01.19.524818> (2023).
40. Karapanagiotidis, T. et al. The psychological correlates of distinct neural states occurring during wakeful rest. *Sci. Rep.* **10**, 21121. <https://doi.org/10.1038/s41598-020-77336-z> (2020).
41. Gonzalez-Castillo, J. et al. Tracking ongoing cognition in individuals using brief, whole-brain functional connectivity patterns. *Proc. Natl. Acad. Sci. USA* **112**, 8762–8767. <https://doi.org/10.1073/pnas.1501242112> (2015).
42. Shirer, W. R. et al. Decoding subject-driven cognitive states with whole-brain connectivity patterns. *Cereb. Cortex* **22**, 158–165. <https://doi.org/10.1093/cercor/bhr099> (2012).
43. Vatansever, D. et al. Distinct patterns of thought mediate the link between brain functional connectomes and well-being. *Netw. Neurosci.* **4**(3), 637–657 (2020). https://doi.org/10.1162/netn_a_00137
44. Gonzalez-Castillo, J. et al. In-Scanner thoughts shape resting-state functional connectivity: How participants rest matters. *Preprint At* <https://doi.org/10.1101/2024.06.05.596482> (2024).
45. Kucyi, A. et al. Spontaneous cognitive processes and the behavioral validation of time-varying brain connectivity. *Netw. Neurosci.* **2**, 397–417 (2018). https://doi.org/10.1162/netn_a_00037
46. Sporns, O. Network attributes for segregation and integration in the human brain. *Curr. Opin. Neurobiol.* **23**, 162–171. <https://doi.org/10.1016/j.conb.2012.11.015> (2013).
47. Cremona, S., Joliot, M. & Mellet, E. Cluster-based characterization of consistencies in individuals' thought profiles at rest in a cohort of 1779 French university students. *Curr. Psychol.* **42**, 31667–31686. <https://doi.org/10.1007/s12144-022-04185-6> (2023).
48. Gorgolewski, K. J. et al. A correspondence between individual differences in the brain's intrinsic functional architecture and the content and form of Self-Generated thoughts. *PLoS ONE* **9**, e97176. <https://doi.org/10.1371/journal.pone.0097176> (2014).
49. Wang, H. T. et al. Patterns of thought: population variation in the associations between large-scale network organisation and self-reported experiences at rest. *NeuroImage* **176**, 518–527. <https://doi.org/10.1016/j.neuroimage.2018.04.064> (2018).
50. Laumann, T. O., Snyder, A. Z. & Gratton, C. Challenges in the measurement and interpretation of dynamic functional connectivity. *Imaging Neurosci.* **2**, 1–19 (2024) https://doi.org/10.1162/imag_a_00366
51. Murphy, K. & Fox, M. D. Towards a consensus regarding global signal regression for resting state functional connectivity MRI. *NeuroImage* **154**, 169–173. <https://doi.org/10.1016/j.neuroimage.2016.11.052> (2017).
52. Zarei, M. et al. High activity and high functional connectivity are mutually exclusive in resting state zebrafish and human brains. *BMC Biol.* **20**, 84. <https://doi.org/10.1186/s12915-022-01286-3> (2022).
53. Ito, T. et al. Task-evoked activity quenches neural correlations and variability across cortical areas. *PLoS Comput. Biol.* **16**, e1007983. <https://doi.org/10.1371/journal.pcbi.1007983> (2020).
54. Gonzalez-Castillo, J. & Bandettini, P. A. Task-based dynamic functional connectivity: Recent findings and open questions. *NeuroImage* **180**, 526–533. <https://doi.org/10.1016/j.neuroimage.2017.08.006> (2018).
55. Shine, J. M. et al. The dynamics of functional brain networks: integrated network states during cognitive task performance. *Neuron* **92**, 544–554. <https://doi.org/10.1016/j.neuron.2016.09.018> (2016).
56. Cole, M. W. et al. Activity flow over resting-state networks shapes cognitive task activations. *Nat. Neurosci.* **19**, 1718–1726. <https://doi.org/10.1038/nn.4406> (2016).
57. Allen, E. A. et al. Tracking whole-brain connectivity dynamics in the resting state. *Cereb. Cortex* **24**, 663–676. <https://doi.org/10.1093/cercor/bhs352> (2014).
58. Deco, G., Jirsa, V. K. & McIntosh, A. R. Emerging concepts for the dynamical organization of resting-state activity in the brain. *Nat. Rev. Neurosci.* **12**, 43–56. <https://doi.org/10.1038/nrn2961> (2011).
59. Zalesky, A. et al. Time-resolved resting-state brain networks. *Proc. Natl. Acad. Sci. U S A* **111**, 10341–10346. <https://doi.org/10.1073/pnas.1400181111> (2014).
60. Yarkoni, T., Poldrack, R. A. & Nichols, T. E. Large-scale automated synthesis of human functional neuroimaging data. *Nat. Methods* **8**, 665–672 (2011). <https://doi.org/10.1038/nmeth.1635>
61. Lynch, L. K. et al. Task-evoked functional connectivity does not explain functional connectivity differences between rest and task conditions. *Hum. Brain. Mapp.* **39**, 4939–4948. <https://doi.org/10.1002/hbm.24335> (2018).
62. Tomasi, D. et al. Functional connectivity and brain activation: A synergistic approach. *Cereb. Cortex* **24**, 2619–2629. <https://doi.org/10.1093/cercor/bht119> (2014).
63. Xu, X., Yuan, H. & Lei, X. Activation and connectivity within the default mode network contribute independently to Future-Oriented thought. *Sci. Rep.* **6**, 21001. <https://doi.org/10.1038/srep21001> (2016).
64. Sormaz, M. et al. Default mode network can support the level of detail in experience during active task States. *Proc. Natl. Acad. Sci. U S A* **115**, 9318–9323. <https://doi.org/10.1073/pnas.1721259115> (2018).
65. Schurz, M. et al. Fractionating theory of mind: A meta-analysis of functional brain imaging studies. *Neurosci. Biobehavioral Reviews* **42**, 9–34. <https://doi.org/10.1016/j.neubiorev.2014.01.009> (2014).
66. Wang, K. et al. Spontaneous activity associated with primary visual cortex: A Resting-State fMRI study. *Cereb. Cortex* **18**, 697–704. <https://doi.org/10.1093/cercor/bhm105> (2008).
67. Zhang, Z. et al. Intrinsic neural linkage between primary visual area and default mode network in human brain: evidence from visual mental imagery. *Neuroscience* **379**, 13–21. <https://doi.org/10.1016/j.neuroscience.2018.02.033> (2018).
68. Orwig, W. et al. Creative connections: computational semantic distance captures individual creativity and resting-state functional connectivity. *J. Cogn. Neurosci.* **33**, 499–509. https://doi.org/10.1162/jocn_a_01658 (2021).
69. Cui, X. et al. Vividness of mental imagery: individual variability can be measured objectively. *Vision. Res.* **47**, 474–478. <https://doi.org/10.1016/j.visres.2006.11.013> (2007).
70. Wood, J. L. & Nee, D. E. Cingulo-opercular subnetworks motivate frontoparietal subnetworks during distinct cognitive control demands. *J. Neurosci.* **43**, 1225–1237. <https://doi.org/10.1523/JNEUROSCI.1314-22.2022> (2023).
71. Newbold, D. J. et al. Cingulo-opercular control network and disused motor circuits joined in standby mode. *Proc. Natl. Acad. Sci. U.S.A.* **118**, e2019128118. <https://doi.org/10.1073/pnas.2019128118> (2021).
72. Beaty, R. E. et al. Default and executive network coupling supports creative idea production. *Sci. Rep.* **5**, 10964. <https://doi.org/10.1038/srep10964> (2015).
73. Beaty, R. E. et al. Robust prediction of individual creative ability from brain functional connectivity. *Proc. Natl. Acad. Sci. U.S.A.* **115**, 1087–1092. <https://doi.org/10.1073/pnas.1713532115> (2018).
74. Bendetowicz, D. et al. Two critical brain networks for generation and combination of remote associations. *Brain* **141**, 217–233. <https://doi.org/10.1093/brain/awx294> (2018).
75. Ellamil, M. et al. Evaluative and generative modes of thought during the creative process. *NeuroImage* **59**, 1783–1794. <https://doi.org/10.1016/j.neuroimage.2011.08.008> (2012).
76. Andrews-Hanna, J. R., Smallwood, J. & Spreng, R. N. The default network and self-generated thought: component processes, dynamic control, and clinical relevance. *Ann. N. Y. Acad. Sci.* **1316**, 29–52. <https://doi.org/10.1111/nyas.12360> (2014).
77. Ekstrom, A. D., Arnold, A. E. G. F. & Iaria, G. A critical review of the allocentric spatial representation and its neural underpinnings: toward a network-based perspective. *Front Hum. Neurosci.* **8**, 803. <https://doi.org/10.3389/fnhum.2014.00803> (2014).
78. Schurz, M., Maliske, L. & Kanske, P. Cross-network interactions in social cognition: A review of findings on task related brain activation and connectivity. *Cortex* **130**, 142–157. <https://doi.org/10.1016/j.cortex.2020.05.006> (2020).
79. Dixon, M. L. et al. Interactions between the default network and dorsal attention network vary across default subsystems, time, and cognitive states. *NeuroImage* **147**, 632–649. <https://doi.org/10.1016/j.neuroimage.2016.12.073> (2017).

80. Derbie, A. Y. et al. Common and distinct neural trends of allocentric and egocentric spatial coding: an ALE meta-analysis. *Eur. J. Neurosci.* **53**, 3672–3687. <https://doi.org/10.1111/ejn.15240> (2021).
81. Keen, S. A theory of narrative empathy. *Narrative* **14**, 207–236 (2006).
82. Shi, Y. *First-Person Narrative and Story Meaningfulness: Promoting Empathy via Storytelling* (University of Chicago, 2021).
83. Kamps, F. S., Lall, V. & Dilks, D. D. The occipital place area represents first-person perspective motion information through scenes. *Cortex* **83**, 17–26. <https://doi.org/10.1016/j.cortex.2016.06.022> (2016).
84. Bergmann, J. et al. Smaller primary visual cortex is associated with stronger, but less precise mental imagery. *Cereb. Cortex* **26**, 3838–3850. <https://doi.org/10.1093/cercor/bhv186> (2016).
85. Pearson, J. et al. Mental imagery: functional mechanisms and clinical applications. *Trends Cogn. Sci.* **19**, 590–602. <https://doi.org/10.1016/j.tics.2015.08.003> (2015).
86. Deck, B. L. et al. Individual-level functional connectivity predicts cognitive control efficiency. *NeuroImage* **283**, 120386. <https://doi.org/10.1016/j.neuroimage.2023.120386> (2023).
87. Kucyi, A. & Davis, K. D. Dynamic functional connectivity of the default mode network tracks daydreaming. *NeuroImage* **100**, 471–480. <https://doi.org/10.1016/j.neuroimage.2014.06.044> (2014).
88. Kucyi, A. et al. Prediction of stimulus-independent and task-unrelated thought from functional brain networks. *Nat. Commun.* **12**, 1793. <https://doi.org/10.1038/s41467-021-22027-0> (2021).
89. Tsuchida, A. et al. The MRI-share database: brain imaging in a cross-sectional cohort of 1870 university students. *Brain Struct. Funct.* **226**, 2057–2085 (2021).
90. Suzuki, R. & Shimodaira, H. Pvcust: an R package for assessing the uncertainty in hierarchical clustering. *Bioinformatics* **22**, 1540–1542. <https://doi.org/10.1093/bioinformatics/btl117> (2006).
91. Lipkin, B. et al. Probabilistic atlas for the language network based on precision fMRI data from > 800 individuals. *Sci. Data* **9**, 529. <https://doi.org/10.1038/s41597-022-01645-3> (2022).
92. Amodio, D. M. & Frith, C. D. Meeting of minds: the medial frontal cortex and social cognition. *Nat. Rev. Neurosci.* **7**, 268–277. <https://doi.org/10.1038/nrn1884> (2006).
93. De La Vega, A. et al. Large-scale meta-analysis of human medial frontal cortex reveals tripartite functional organization. *J. Neurosci.* **36**, 6553–6562. <https://doi.org/10.1523/JNEUROSCI.4402-15.2016> (2016).
94. Thye, M., Hoffman, P. & Mirman, D. The neural basis of naturalistic semantic and social cognition. *Sci. Rep.* **14**, 6796. <https://doi.org/10.1038/s41598-024-56897-3> (2024).
95. Gough, P. M., Nobre, A. C. & Devlin, J. T. Dissociating linguistic processes in the left inferior frontal cortex with transcranial magnetic stimulation. *J. Neurosci.* **25**, 8010–8016. <https://doi.org/10.1523/JNEUROSCI.2307-05.2005> (2005).
96. Herlin, B., Navarro, V. & Dupont, S. The temporal pole: from anatomy to function—A literature appraisal. *J. Chem. Neuroanat.* **113**, 101925. <https://doi.org/10.1016/j.jchemneu.2021.101925> (2021).
97. Igelström, K. M. & Graziano, M. S. A. The inferior parietal lobule and temporoparietal junction: A network perspective. *Neuropsychologia* **105**, 70–83. <https://doi.org/10.1016/j.neuropsychologia.2017.01.001> (2017).
98. Oberhuber, M. et al. Four functionally distinct regions in the left supramarginal gyrus support word processing. *Cereb. Cortex* **26**, 4212–4226. <https://doi.org/10.1093/cercor/bhw251> (2016).
99. Wada, S. et al. Volume of the right supramarginal gyrus is associated with a maintenance of emotion recognition ability. *PLoS ONE* **16**, e0254623. <https://doi.org/10.1371/journal.pone.0254623> (2021).
100. Paunov, A. M., Blank, I. A. & Fedorenko, E. Functionally distinct Language and theory of Mind networks are synchronized at rest and during language comprehension. *J. Neurophysiol.* **121**, 1244–1265. <https://doi.org/10.1152/jn.00619.2018> (2019).
101. Buckner, R. L., Andrews-Hanna, J. R. & Schacter, D. L. The brain's default network: anatomy, function, and relevance to disease. *Ann. N. Y. Acad. Sci.* **1124**, 1–38. <https://doi.org/10.1196/annals.1440.011> (2008).
102. Sandhu, Z. et al. Parcellation-based anatomic modeling of the default mode network. *Brain Behav.* **11**, e01976. <https://doi.org/10.1002/brb3.1976> (2021).
103. Wang, X. et al. Anterior insular cortex plays a critical role in interoceptive attention. *eLife* **8**, e42265. <https://doi.org/10.7554/eLife.e42265> (2019).
104. Craig, A. D. Bud. How do you feel — now? The anterior Insula and human awareness. *Nat. Rev. Neurosci.* **10**, 59–70. <https://doi.org/10.1038/nrn2555> (2009).
105. Gu, X. et al. Anterior insular cortex and emotional awareness. *J. Comp. Neurol.* **521**, 3371–3388. <https://doi.org/10.1002/cne.23368> (2013).
106. Dosenbach, N. U. F., Raichle, M. & Gordon, E. M. The brain's cingulo-opercular action-mode network. *Nat. Rev. Neurosci.* **26**(3), 158–168. <https://doi.org/10.1038/s41583-024-00895-x> (2025).
107. Cignetti, F. et al. Brain network connectivity associated with anticipatory postural control in children and adults. *Cortex* **108**, 210–221. <https://doi.org/10.1016/j.cortex.2018.08.013> (2018).
108. Corbetta, M., Patel, G. & Shulman, G. L. The reorienting system of the human brain: from environment to theory of mind. *Neuron* **58**, 306–324. <https://doi.org/10.1016/j.neuron.2008.04.017> (2008).
109. Yamaguchi, A. & Jitsuiishi, T. Structural connectivity of the precuneus and its relation to resting-state networks. *Neurosci. Res.* <https://doi.org/10.1016/j.neures.2023.12.004> (2023).
110. Ramezanzpour, H. & Fallah, M. The role of temporal cortex in the control of attention. *Curr. Res. Neurobiol.* **3**, 100038 (2022). <https://doi.org/10.1016/j.crneur.2022.100038>
111. Sani, I. et al. The human endogenous attentional control network includes a ventro-temporal cortical node. *Nat. Commun.* **12**, 360. <https://doi.org/10.1038/s41467-020-20583-5> (2021).
112. Zhang, W. et al. Functional organization of the fusiform gyrus revealed with connectivity profiles. *Hum. Brain. Mapp.* **37**, 3003–3016. <https://doi.org/10.1002/hbm.23222> (2016).
113. Vossel, S., Geng, J. J. & Fink, G. R. Dorsal and ventral attention systems: distinct neural circuits but collaborative roles. *Neuroscientist* **20**, 150–159. <https://doi.org/10.1177/1073858413494269> (2014).
114. Ptak, R. The frontoparietal attention network of the human brain: action, saliency, and a priority map of the environment. *Neuroscientist* **18**, 502–515. <https://doi.org/10.1177/1073858411409051> (2012).
115. Qiu, L. et al. Functional specialization of medial and lateral orbitofrontal cortex in inferential decision-making. *iScience* **27**, 110007. <https://doi.org/10.1016/j.isci.2024.110007> (2024).
116. Rushworth, M. The left parietal cortex and motor attention. *Neuropsychologia* **35**, 1261–1273. [https://doi.org/10.1016/S0028-3932\(97\)00050-X](https://doi.org/10.1016/S0028-3932(97)00050-X) (1997).
117. Canty, A. & Ripley, B. D. boot: Bootstrap R (S-Plus) Functions. (2020).
118. Zhang, C. et al. Sex and age effects of functional connectivity in early adulthood. *Brain Connect.* **6**, 700–713. <https://doi.org/10.1089/brain.2016.0429> (2016).
119. Baguley, T. Standardized or simple effect size: what should be reported?. *Br. J. Psychol.* **100**, 603–617. <https://doi.org/10.1348/000712608X377117> (2009).
120. R Core Team. R: A language and environment for statistical computing (R Foundation for statistical computing, 2020).
121. RStudio Team. RStudio: Integrated development environment for R. RStudio Team. (2020).
122. Kuznetsova, A., Brockhoff, P. B. & Christensen, R. H. B. lmerTest package: Tests in linear mixed effects models. *Journal Stat. Software* **82**, 1–26. <https://doi.org/10.18637/jss.v082.i13> (2017).
123. Lenth, R. V. Package ‘emmeans’. (2020).

Acknowledgements

The authors thank Christophe Tzourio for the project administration and funding acquisition. They thank the 1,870 Bordeaux University students who consented to participate in MRi-Share.

Author contributions

Conceptualization: E.M., M.J., S.C.; Methodology: A.G., M.J., S.C.; Formal analysis: M.J., S.C.; Visualization: M.J., S.C.; Writing—original draft, review, editing: S.C.; Writing—review & editing: A.G., E.M., M.J.

Funding

The i-Share team was supported by a grant from the Nouvelle-Aquitaine Regional Council (Conseil Régional Nouvelle-Aquitaine) (grant N° 4370420) and by the Bordeaux “Initiatives d’excellence” (IdEx) program of the University of Bordeaux (ANR-10IDEX-03–02). It has also received grants from the Nouvelle-Aquitaine Regional Health Agency (Agence Régionale de Santé Nouvelle-Aquitaine) and Public Health France (Santé Publique France). The MRi-Share cohort has been supported by ANR-10LABX-57 (TRAIL) and a grant from the Nouvelle-Aquitaine Regional Council (Conseil Régional Nouvelle-Aquitaine). Achille Gillig has benefited from state support managed by the Agence Nationale de la Recherche (French National Research Agency) under reference 17-EURE-0028.

Declarations

Competing interests

The authors declare no competing interests.

Additional information

Correspondence and requests for materials should be addressed to S.C.

Reprints and permissions information is available at www.nature.com/reprints.

Publisher’s note Springer Nature remains neutral with regard to jurisdictional claims in published maps and institutional affiliations.

Open Access This article is licensed under a Creative Commons Attribution-NonCommercial-NoDerivatives 4.0 International License, which permits any non-commercial use, sharing, distribution and reproduction in any medium or format, as long as you give appropriate credit to the original author(s) and the source, provide a link to the Creative Commons licence, and indicate if you modified the licensed material. You do not have permission under this licence to share adapted material derived from this article or parts of it. The images or other third party material in this article are included in the article’s Creative Commons licence, unless indicated otherwise in a credit line to the material. If material is not included in the article’s Creative Commons licence and your intended use is not permitted by statutory regulation or exceeds the permitted use, you will need to obtain permission directly from the copyright holder. To view a copy of this licence, visit <http://creativecommons.org/licenses/by-nc-nd/4.0/>.

© The Author(s) 2025